Aaryan Kulkarni, Vesapogu Sujana Deepthi, Nishant Kumar, Sridhar Miriyala* and Devanaboyina Venkata Ratnam

Statistical analysis of Precipitable Water Vapor and rainfall variability in different geographical conditions of the Indian region

https://doi.org/10.1515/jag-2025-0019
Received February 10, 2025; accepted May 22, 2025;
published online June 25, 2025

Abstract: Monitoring Precipitable Water Vapor (PWV) with Global Navigation Satellite System (GNSS) receivers is becoming a more viable and effective solution for meteorological applications such as rainfall prediction, climate change, and weather forecasting etc. This study investigates the statistical relationship between GNSS-derived Precipitable Water Vapor (PWV) and rainfall variability across five Indian cities, Bangalore, Hyderabad, Guwahati, Thiruvananthapuram, and Madurai, representing diverse geographic and climatic zones. GNSS-derived PWV data from the GPS Aided Geo Augmented Navigation (GAGAN) network and rainfall data from the Indian Meteorological Department (IMD) were considered from March 2013 to February 2014. Data has been analyzed based on seasonal trends and the dynamic interaction between atmospheric moisture and precipitation. The results represented significant spatial and temporal differences in rainfall patterns, with Thiruvananthapuram recording the highest monthly rainfall (143.90 mm in October 2013) due to dual monsoon exposure, and Madurai the lowest (88.5 mm in October 2013) owing to its rain-shadow location. Guwahati shows strong orographic influence and early monsoon peaks (121.30 mm in June 2013), while inland cities like Bangalore and Hyderabad experience delayed rainfall peaks during post-monsoon periods. Average monthly rainfall and PWV values were found to be closely linked to geographical factors such as elevation, topography, and proximity to coastlines. A clear correlation was observed between PWV and subsequent rainfall events; sharp increases in PWV exceeding 30 mm daily or rising at rates above 0.5 mm/h often preceded heavy precipitation.

***Corresponding author: Sridhar Miriyala**, Koneru Lakshmaiah Education Foundation (Deemed to be University), Guntur, 522302, India, E-mail: sridhar.m@kluniversity.in
Aaryan Kulkarni, **Vesapogu Sujana Deepthi**, **Nishant Kumar** and **Devanaboyina Venkata Ratnam**, Koneru Lakshmaiah Education Foundation (Deemed to be University), Guntur, 522302, India

Keywords: Precipitable Water Vapor; GNSS; rainfall; diurnal variations

1 Introduction

Our Earth's atmosphere contains water vapor, one of the main elements that helps form clouds and precipitation. It plays an influential role in several atmospheric processes, including rainfall variability and global climate. Precipitation is essential to the worldwide water cycle as heavy rainfall can affect the natural environment, social life, and result in economic harm. It is the most fluctuating of all the main components of the atmosphere that plays a key role in the Earth's water and energy cycles and has a greater impact on the greenhouse effect [1–3]. Precipitable Water Vapor (PWV), derived from the GNSS network, is the quantity of water in an imaginary vertical column with a unit area of cross-section from the Earth's surface to the atmosphere that can be utilized for precipitation [4–8]. The change in PWV, observed with high accuracy and precision in time series, can be used to predict rainfall and other severe weather events [9]. On analyzing the dissimilarities of the water vapor, the PWV derived from GNSS can be considered an important factor for the inflow and outflow of water vapor in the vertical air column of a specific area [10, 11]. Radiosonde, weather radar, and ground-based radiometers are used for estimating PWV [12–16]. Many studies have examined GNSS-derived PWV's ability to predict rainfall, establishing a relationship between PWV and rainfall [17]. It is further verified that the probability of a rainfall event significantly increases when PWV exceeds a certain threshold level [12, 13].

Bevis et al. (1992) introduced GPS meteorology by experimentally organizing a utility for using GPS to measure water vapor [1]. GNSS-based methods include GPS and offer continuous advantages and worthwhile procedures under all weather conditions, providing PWV data with high continuity and integrity. Researchers have demonstrated that GPS-based PWV measurements, compared to water vapor radiometers and radiosondes, can achieve an RMSE of 1–2 mm [18–21]. The expanding research of GNSS-based PWV has opened new challenges for global-scale PWV monitoring, supported by extensive databases like the Nevada Geodetic Laboratory's troposphere products, which are now available for such analyses.

Multiple researchers have demonstrated the capability of utilizing GPS to ascertain the integrated quantity of water vapor in the atmosphere. There is a high degree of agreement between PWV measured by the International GNSS Service (IGS) Multi-GNSS Experiment (MGEX) and PWV measured by various instruments (e.g., BeiDou, Galileo, GLONASS, and GPS) [22]. Rivera et al. (2021) presented the fluctuations and patterns of PWV across four Philippine stations (Laoag, Legazpi, Mactan, and Puerto Princesa) spanning the years 2012–2019 [23]. Domingo and Macalalad (2020) illustrated the fluctuations in PWV over Tanay Station from 2015 to 2017 by utilizing data obtained from radiosondes, GNSS, and rainfall data, and observed that PWV values were satisfactory in both dry and rainy seasons [24]. May to October is its zenith, while November to April is its minimum. Conversely, it was observed that the dry season exhibited significant variability, whereas the rainy season displayed minimal variability. Nevertheless, there appears to be a nascent stage to developing algorithms specifically designed for diverse geographic regions and the spatiotemporal analysis of PWV derived from GNSS.

Saha et al. (2010) introduced a novel hydrostatic mapping function for accurately estimating tropospheric delay [25]. The model effectively predicts both short-term and long-term ionospheric delays, which are challenging due to varying solar and geomagnetic conditions. Using GPS measurements, Nirmala et al. (2020) conducted a study on the fluctuations of integrated water vapor in Hyderabad, a tropical station. The study examined the yearly, seasonal, and diurnal changes of integrated water vapor [26].

There is a need for a complete understanding of the spatiotemporal features of the PWV for improving accurate prediction of weather patterns, and locating climate change

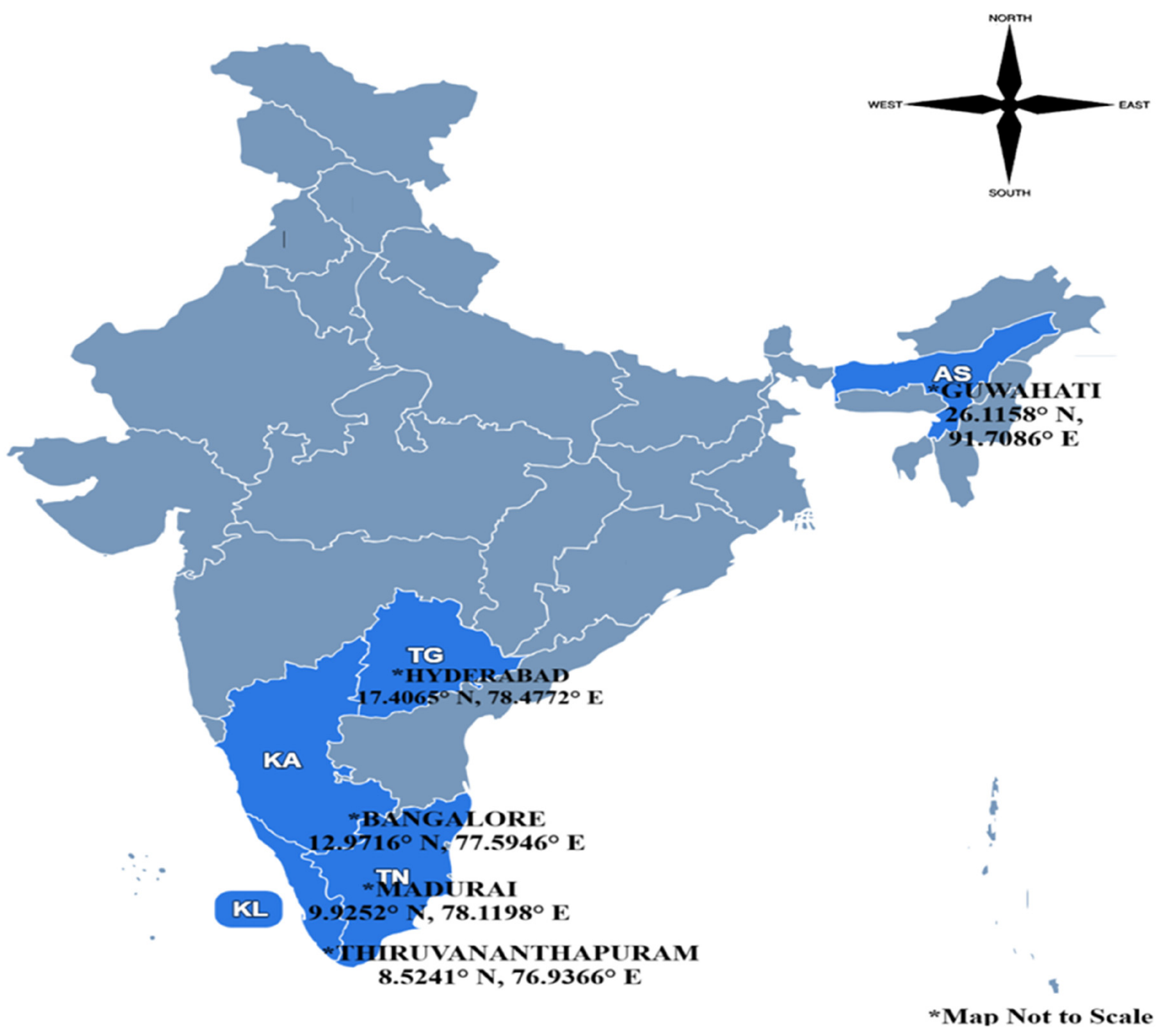

Figure 1: Geographical topography of selected locations.

problems efficiently. In this research, a correlational examination of rainfall events over the Indian subcontinent is conducted by evaluating the similarity between PWV and seasonal, intraseasonal, diurnal, and rainfall. The relationship between rainfall rate data and PWV data was also examined, and correlation analysis was conducted for several severe rainfall events observed over the study area.

2 Study area(s)

This study focuses on five different cities across India, each having different geographic conditions. Bangalore, located at 12.97° N, 77.56° E on the Mysore Plateau, is a landlocked city with an elevation of 920 m and has an area of 741 Km^2. Hyderabad, located at 17.366° N, 78.476° E in the Deccan Plateau, which is also a landlocked city, with an elevation of 524 m and has an area of 650 Km^2. Guwahati, located at 26.11° N, 91.71° E, lies between the banks of the Brahmaputra River and the foothills of the Shillong Plateau, featuring a hilly terrain with an elevation ranging from 50 to 680 m has an area of 216 Km^2. Thiruvananthapuram, located at 8.5° N, 76.9° E along the western coast, is a coastal city with an elevation of 33.93 m and has an area of 214 Km^2. Madurai, located at 9.92° N, 78.12° E, is a landlocked city having flat plains, with an average elevation of 134 m, and has an area of 147.97 Km^2. These cities were selected on the availability of co-located GAGAN GPS receivers derived PWV and IMD rainfall data are analyzed to cover a range of geographical and climatic conditions across India, ranging from plateau (Bangalore, Hyderabad), coastal (Thiruvananthapuram), hilly (Guwahati), to inland plains (Madurai). They span latitudes from 8.5°N to 26.1°N and longitudes from 76.9°E to 91.7°E, providing a representative sample for analyzing spatial variability of Precipitable Water Vapor and rainfall in different environmental settings. The availability of co-located GAGAN GPS receivers and IMD weather stations further supported their selection (Figure 1).

2.1 Data collection

This GAGAN PWV dataset includes estimates of Integrated Water Vapour (IWV) obtained from GPS receivers that is part of the GAGAN TEC network over the Indian region. These receivers have been deployed at many sites throughout India's airports. The GAGAN-IWV estimations for a duration of one year, namely from March 2013 to February 2014, are presently accessible. The rainfall data is obtained from the Indian Meteorological Department for the same time intervals. Although the analysis is based on a relatively short-term dataset, this period covers seasonal cycles pre-monsoon, monsoon, post-monsoon, and winter, which are critical for understanding the short-term variability and relationship between PWV and rainfall. The period was also selected due to the availability of consistent, high-quality data from the GAGAN GPS receivers and IMD stations during this phase.

3 GNSS PWV

The Precipitable Water Vapor (PWV) values are derived using Global Navigation Satellite System (GNSS) data from the GAGAN (GPS Aided GEO Augmented Navigation) network. GAGAN is a joint initiative of the Indian Space Research Organization (ISRO) and the Airports Authority of India (AAI), with GNSS receivers deployed at various Indian airports. GNSS data for the period March 2013 to February 2014 were obtained from the ISRO data (Table 1). This dataset contains Integrated Water Vapor (IWV) estimates derived from GPS receivers that comprise the GAGAN TEC network. Daily rainfall data for the same period (March 2013 to February 2014) were acquired from the Indian Meteorological Department (IMD), which maintains a nationwide network of surface observatories. The rainfall data corresponding to the nearest IMD station for each selected city were used. Daily values were aggregated into monthly totals for trend analysis and event-specific time series for correlation with PWV.

The Zenith Tropospheric Delay (ZTD) is a parameter obtained by the delay of the GNSS signal of a satellite in the lower altitude atmosphere layer, which can be divided in two major components, i.e. the hydrostatic and the wet delay [24]. ZTD is known as the averaged value of the delay of the GNSS satellite network for different signals captured at the same receiver, which can be expressed as:

$$\mathrm{ZTD} = \mathrm{ZHD} + \mathrm{ZWD} \tag{1}$$

where ZTD is the Zenith Total Delay, ZHD is the Zenith Hydrostatic Delay, which has a composition of nearly 80–90 % of ZTD, highly affected by the latitude of the observed station and the surface pressure. ZWD is Zenith Wet Delay, which has a composition of nearly 10–20 % of ZTD. This factor affects the signal of satellites due to the change in movements of the poles of water vapor molecules and is highly similar to water vapor concentration [25].

3.1 Estimation of PWV

PWV is generally expressed in kg m^{-2}. The relation of PWV and ZWD is given in the following equation [27]:

Table 1: PWV, rainfall, and cities data details.

Dataset	Temporal resolution	Spatial resolution	Source URL	Purpose in study
GAGAN GNSS	30 min averaged data	Point-based (airport stations)	https://www.mosdac.gov.in/gps-derived-integrated-water-vapour	PWV estimation
IMD daily rainfall	Hourly data	Point-based (city stations)	https://mausam.imd.gov.in/responsive/rainfallinformation_swd.php	Rainfall analysis and correlation with PWV
City topographical parameters	Static	City-scale	https://www.surveyofindia.gov.in/documents/soichapter-xi.pdf	Classification of geographical features and elevations

$$\mathrm{PWV} = \Pi * \mathrm{ZWD} \tag{2}$$

Π is the conversion factor. It is expressed as,

$$\Pi = \frac{10^6}{\left(k_2' + k_3/T_m\right) \cdot R_v \cdot \rho} \tag{3}$$

where, $k_2 = 16.48\ \mathrm{K} \cdot \mathrm{hPa}^{-1}$

$$k_3 = (3.776 \pm 0.014) \times 10^5\ \mathrm{K}^2\ \mathrm{hP} \cdot \mathrm{a}^{-1}$$

Here, $k_2$and k_3 are the constants

$R\omega = 461\left(J \cdot \mathrm{kg}^{-1}\mathrm{K}^{-1}\right)$which is the gas constant (ideal) for water vapor

ρ is the density of the water vapour, T_m is the mean temperature of the atmospheric column.

$T_m = 0.6066 \cdot T_s + 113.2914$, for daytime

$T_m = 0.7938 \cdot T_s + 57.4856$, for nighttime, Here, T_s is the surface temperature in Kelvin.

3.2 Change in PWV (ΔPWV)

Observing and analyzing the change in PWV is very important for rainfall predictions. PWV values rise significantly just before a rainfall event and then a declining trend is observed in the PWV values, and generally, rainfall occurs at the peak value of the PWV [28, 29]. Therefore, observing the change in PWV factor is very important in predicting rainfall [30]. Now, we define a few other parameters to establish the relationship between PWV and rainfall, such as [4]:

- ΔPWV (Variation in PWV): It is the difference between the maximum PWV and the minimum PWV, the maximum PWV taken before rainfall event and subsequent the minimum PWV after the peak of the PWV values.
- Interval epoch (h): It represents the time interval in hours of the maximum and minimum PWV observed.

The rate of PWV change can then be expressed as the ratio of ΔPWV to h (interval epoch).

4 Results and discussion

4.1 Monthly and seasonal variation of PWV

Figure 2 and Table 2 illustrate the diurnal variation of PWV from March 2013 to February 2014 for five cities: Madurai, Bangalore, Thiruvananthapuram, Hyderabad, and Guwahati, which have distinct geographical factors. Bangalore had moderate PWV levels, which peaked in September 2013 (44.04 ± 1.43 mm) and reached a minimum in December

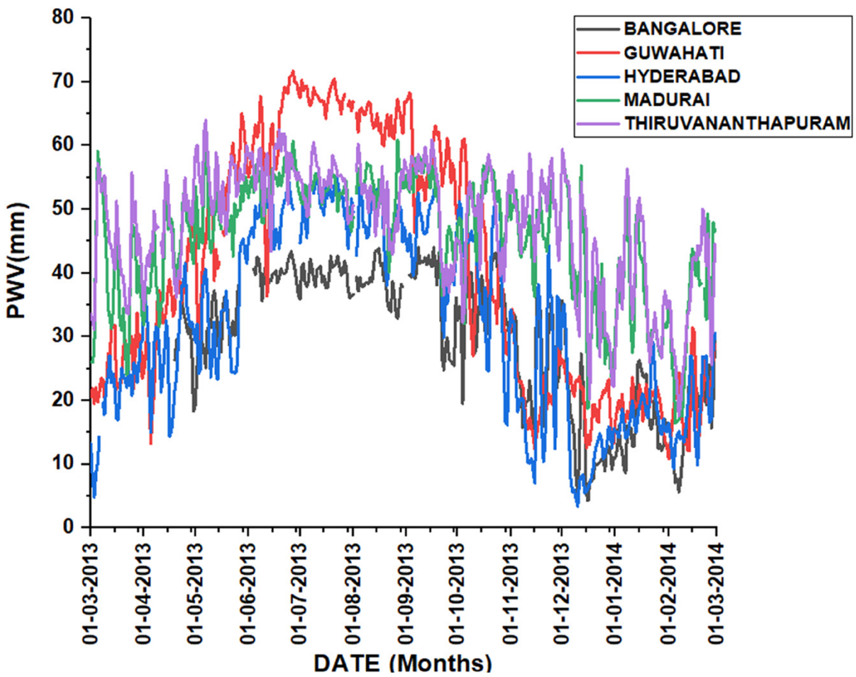

Figure 2: Diurnal PWV variation for the selected 5 cities.

2013 (4.26 ± 1.33 mm), with the average highest diurnal variation in June 2013 (40.02 ± 1.82 mm). Hyderabad showed a steady increase in PWV leading to a peak in July 2013 (56.13 ± 1.88 mm), followed by a minimum in December 2013 (3.39 ± 0.49 mm), with the average highest diurnal variation in July 2013 (51.12 ± 1.78 mm) and the lowest diurnal variation in December 2013 (3.39 ± 0.49 mm). Guwahati recorded the highest PWV in June 2013 (71.68 ± 0.87 mm) and the lowest in February 2014 (10.80 ± 1.46 mm), with the average strongest diurnal variation in July 2013 (67.60 ± 1.71 mm), due to intense monsoon activity and minimum in January 2014 (19.01 ± 2.50). Thiruvananthapuram, being a coastal city, consistently maintained higher moisture levels, with PWV peaked in May 2013 (63.98 ± 1.06 mm) and lowest in February 2014 (17.56 ± 3.68 mm), with the average highest diurnal variation in June 2013 (56.63 ± 4.11 mm) due to pre-monsoon convection and minimum in February 2014 (35.04 ± 11.30 mm). Madurai followed a similar trend as it is situated near the coastline, with maximum PWV in August 2013 (60.82 ± 1.79 mm) and a sharp decline in February 2014 (16.41 ± 1.44 mm), experiencing the highest average diurnal variation in June 2013 (54.46 ± 2.68 mm) and lowest in February 2014 (32.80 ± 10.26 mm). Overall, PWV exhibited a seasonal pattern across all cities, reached peak values during the monsoon months (June to September), and declined post-monsoon (October to December), with coastal regions maintaining higher moisture levels compared to inland locations. The PWV value is higher in coastal areas, Thiruvananthapuram, and Madurai. The seasonal variation of PWV is evident across all stations, with peak values during the monsoon months such as June, July, and August, highlighting the influence of monsoonal moisture influx.

4.2 Monthly variation of rainfall

This section focuses on the monthly rainfall variation and is visualized through a line plot. The plot demonstrates how rainfall (measured in millimeters) changes across different months of the year, allowing us to observe the seasonal rainfall trends. Figure 3 presents the rainfall trends for five selected cities, namely Bangalore, Hyderabad, Guwahati, Thiruvananthapuram, and Madurai from March 2013 to February 2014. These plots provide the temporal distribution of rainfall, highlighting periods of peak and minimal precipitation. Rainfall variability across the selected cities is influenced by a combination of topographic features, proximity to coastlines, elevation, and monsoonal wind dynamics. Coastal Thiruvananthapuram receives high rainfall due to persistent oceanic moisture inflow, while inland Madurai records lower precipitation due to limited moisture access. Guwahati's orographic terrain intensifies rainfall through upslope lifting, whereas plateau cities Hyderabad and Bangalore receive more localized, convective rain. These patterns highlight the complex geographic and atmospheric mechanisms shaping regional precipitation.

Table 2: PWV analysis results for different parameters.

S. no.	City	Diurnal variation of PWV (mm)				Monthly average of PWV (mm)			
		Maximum		Minimum		Maximum		Minimum	
		Value	Month	Value	Month	Value	Month	Value	Month
1	Bangalore	44.04 ± 1.43	September 2013	4.26 ± 1.33	December 2013	40.02 ± 1.82	June 2013	14.32 ± 8.29	December 2013
2	Hyderabad	56.13 ± 1.88	July 2013	3.39 ± 0.49	December 2013	51.12 ± 1.78	July 2013	12.64 ± 8.15	December 2013
3	Guwahati	71.68 ± 0.87	June 2013	10.80 ± 1.46	February 2014	67.60 ± 1.71	July 2013	19.01 ± 2.50	January 2014
4	Thiruvananthapuram	63.98 ± 1.06	May 2013	17.56 ± 3.68	February 2014	56.63 ± 4.11	June 2013	35.04 ± 11.30	February 2014
5	Madurai	60.82 ± 1.79	August 2013	16.41 ± 1.44	February 2014	54.46 ± 2.68	June 2013	32.80 ± 10.26	February 2014

Figure 3 and Table 3 present the rainfall trends for five selected cities from March 2013 to February 2014. These plots provide the temporal distribution of rainfall, highlighting periods of peak and minimal precipitation. The highest recorded monthly rainfall occurred in Thiruvananthapuram (143.90 mm, October 2013), primarily due to its coastal location and exposure to both southwest and northeast monsoons. Guwahati (121.30 mm, June 2013) received substantial rainfall influenced by the Bay of Bengal branch of the southwest monsoon and its proximity to the Eastern Himalayas. Bangalore (108.40 mm, November 2013) and Hyderabad (98.30 mm, October 2013) experienced post-monsoon showers from retreating monsoon currents. Madurai (88.50 mm, October 2013) had the lowest maximum rainfall, as it lies in a rain shadow region and receives limited southwest monsoon influence. The average monthly rainfall relates to the geographical condition of the selected places. Guwahati's peak (11.21 mm, June 2013) results from early monsoon arrival and orographic lifting. Bangalore's lowest (4.79 mm, November 2013) reflects its inland location and weaker retreating monsoon. Moderate values of Hyderabad (7.49 mm, October 2013), Madurai (5.23 mm, October 2013), and Thiruvananthapuram (6.89 mm, October 2013) illustrate the role of local topography and monsoon phase in shaping rainfall intensity.

4.3 Relationship between PWV and rainfall data

The relationship between PWV and rainfall is significant for weather forecasting. Figures 4–8 and Table 4 shown the relationship between PWV and rainfall. It is observed that PWV typically rises before rainfall events and decreases afterward. The peak rainfall often occurs near the PWV peak, establishing a clear correlation. Rapid increases in PWV (ΔPWV) are observed hours before rains, which can be used to predict such events. For instance, Table 4 shows that before the two heaviest rainfall events, PWV levels exceeded 30 mm, sometimes reaching over 70 mm in a single day. PWV variations reached up to 12.6 mm within 8 h, with rates of change above 0.5 mm/h. The differences in PWV and rainfall patterns can be attributed mainly to the cities' geographic characteristics. Guwahati's hilly topography results in orographic enhancement of precipitation during periods of high-water vapor, while coastal Thiruvananthapuram benefits from continuous moisture inflow from the Arabian Sea, sustaining higher baseline PWV. Madurai exhibits lower PWV and reduced rainfall intensities, likely due to its greater distance from oceanic moisture sources and lower elevation. Both Hyderabad and Bangalore, situated on elevated plateaus, showed moderate PWV values

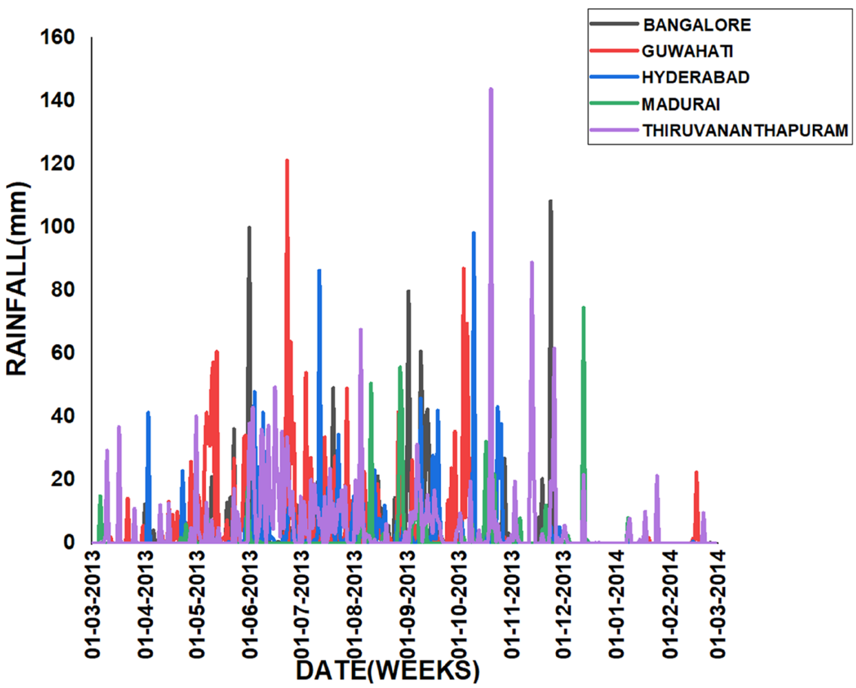

Figure 3: Diurnal Rainfall variation for the selected 5 cities.

Table 3: Rainfall & PWV analysis results for different parameters.

S. no.	City	Month	Maximum rainfall (mm)	Average rainfall (mm)	Minimum PWV (mm)	Maximum PWV (mm)
1	Bangalore	November	108.40	4.79	14.42	36.13
2	Hyderabad	October	98.30	7.49	16.15	52.67
3	Guwahati	June	121.30	11.21	36.34	71.68
4	Thiruvananthapuram	October	143.90	6.89	32.32	58.58
5	Madurai	October	88.5	5.23	32.05	56.91

but differences in rainfall behaviour, attributed to local convective dynamics and urban surface heterogeneities.

In Figures 4–8, the peak values, low values, and changes in PWV were examined before rainfall events (red circles). It can be seen from Table 4 that before rainfall, maximum PWV has reached peak level, and all the values are above 30 mm, and some even reach more than 70 mm on a single day. PWV changes a lot, sometimes reaching 12.6 mm 8 h before rain. Most of the time, the PWV increases at more than 0.5 mm/h. This shows that a quick buildup of GNSS-derived PWV just before rain is for rainfall. The analysis indicates that GNSS-derived PWV and rainfall are correlated, with rain often happening during the rising phase of PWV. This correlation can help in short-term rainfall forecasting. Table 4 denotes the change in PWV values for two heavy rainfall events in the five cities

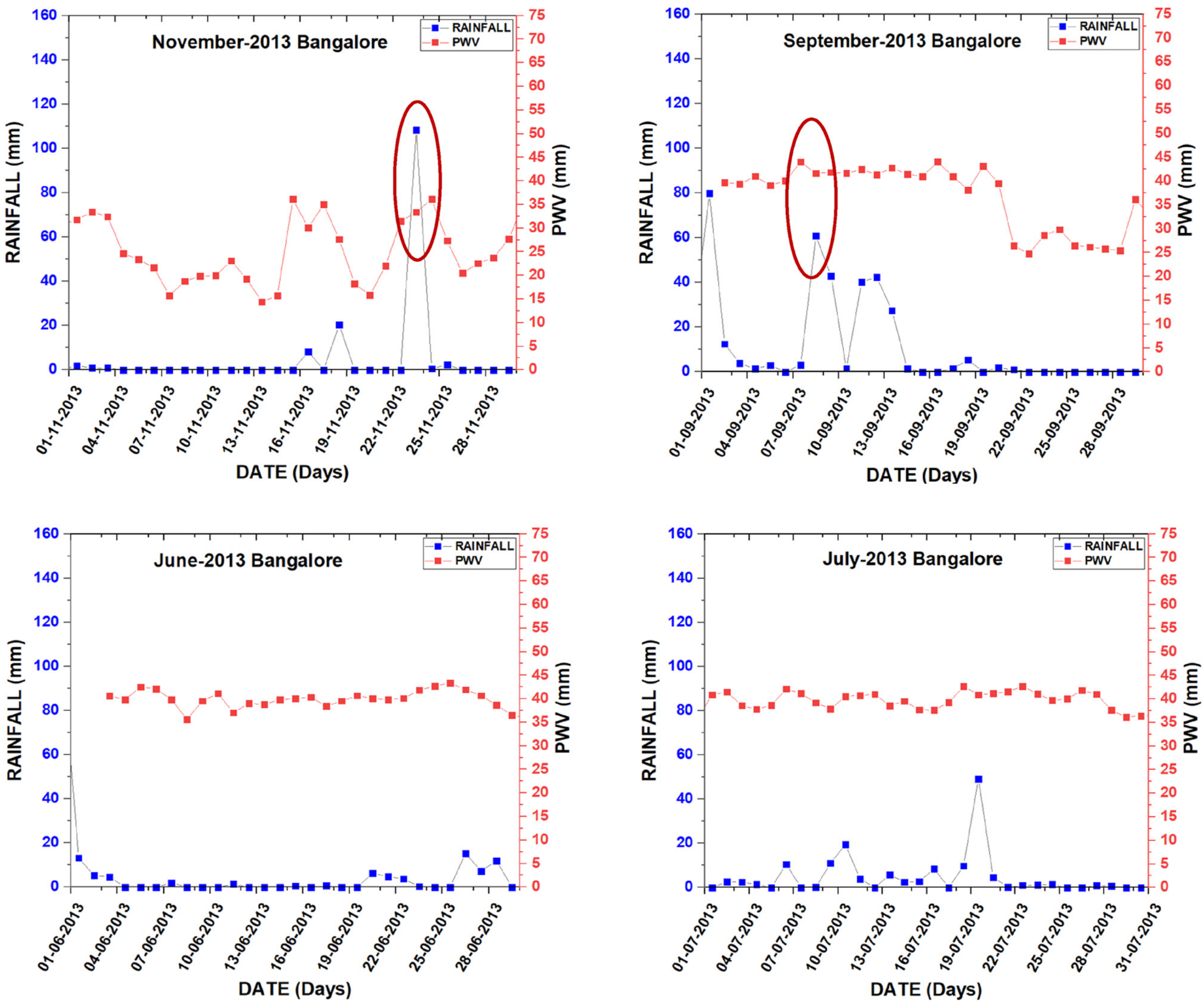

Figure 4: PWV and rainfall variation in Bangalore.

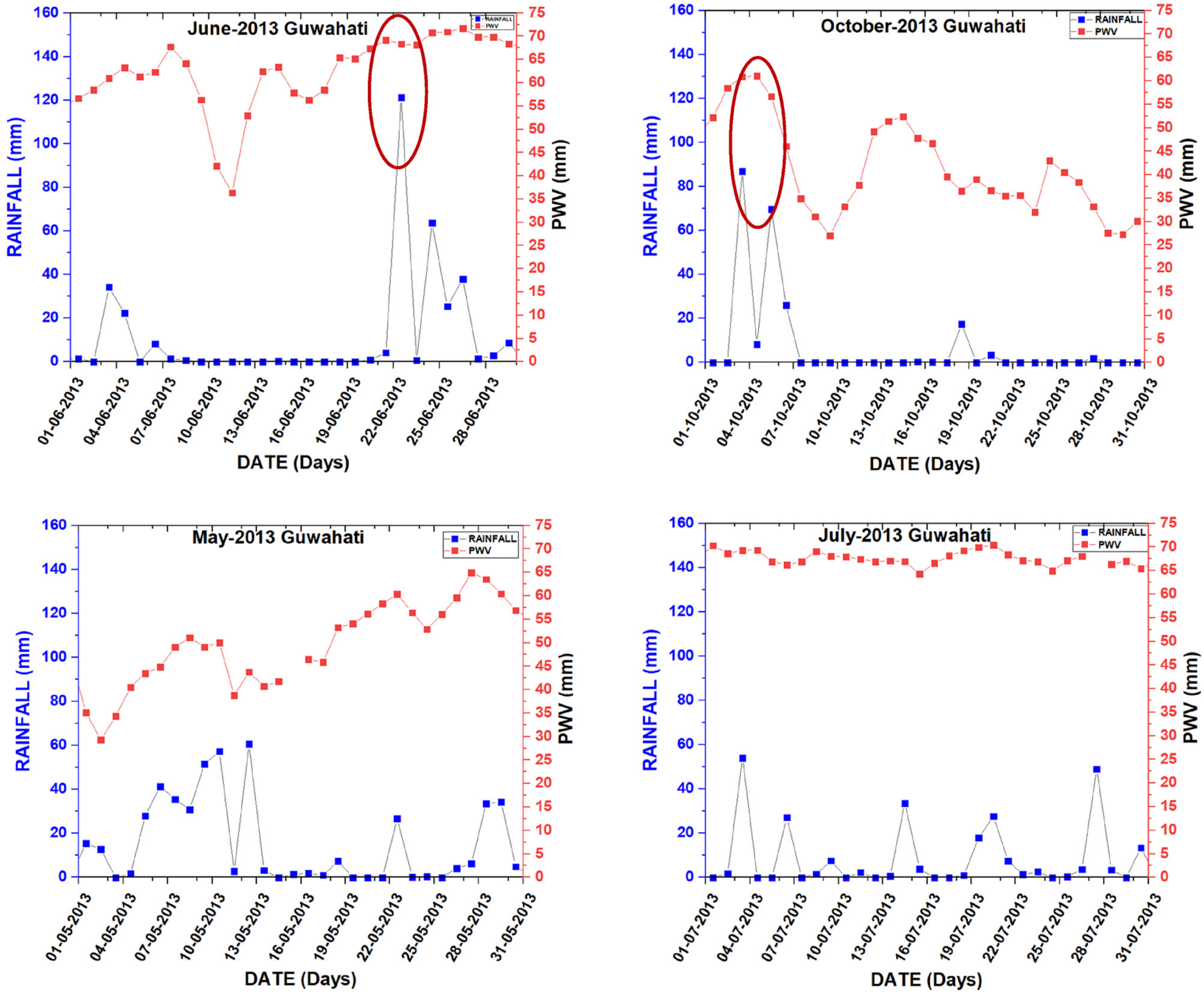

Figure 5: PWV and rainfall variation in Guwahati.

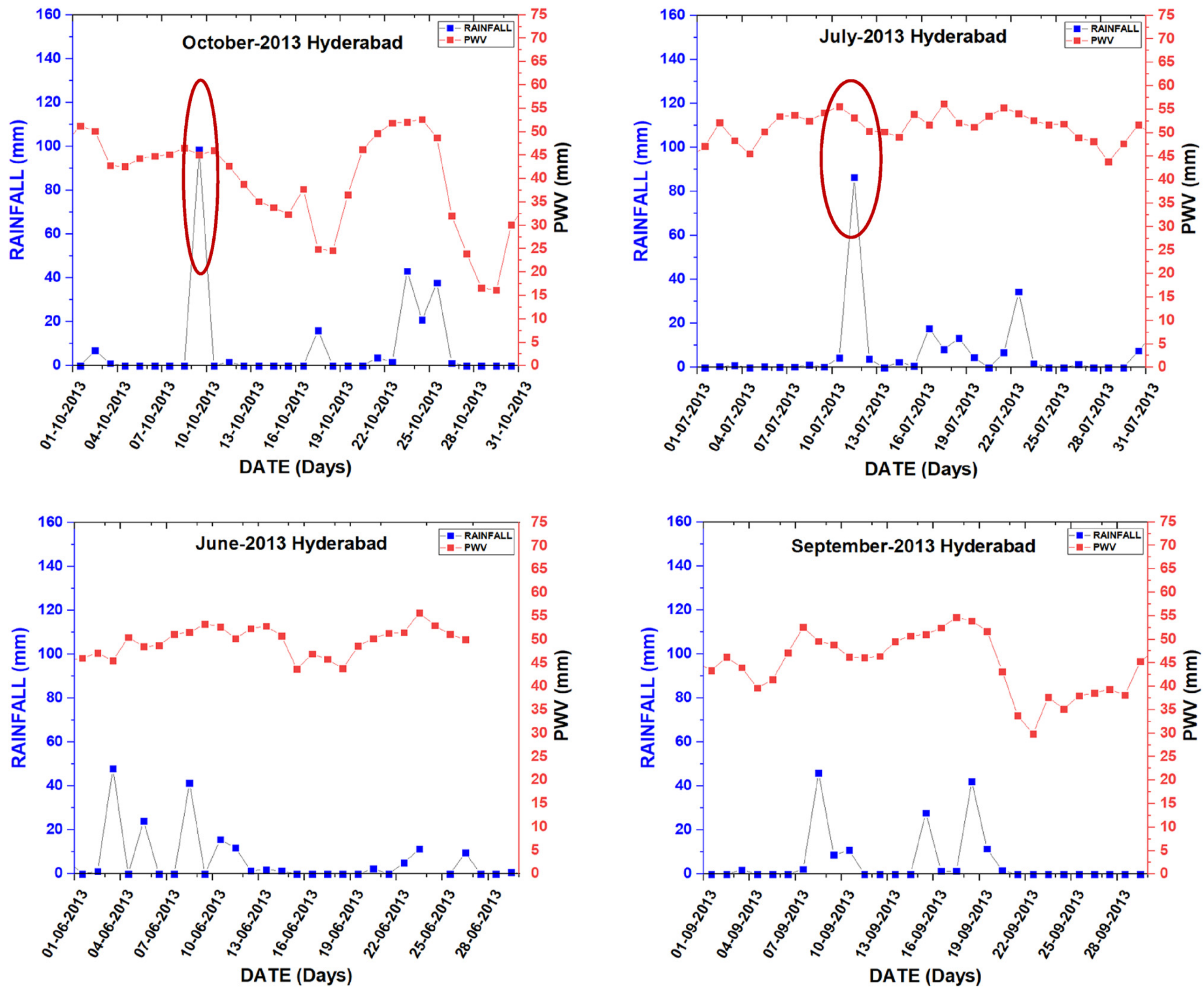

Figure 6: PWV and rainfall variation in Hyderabad.

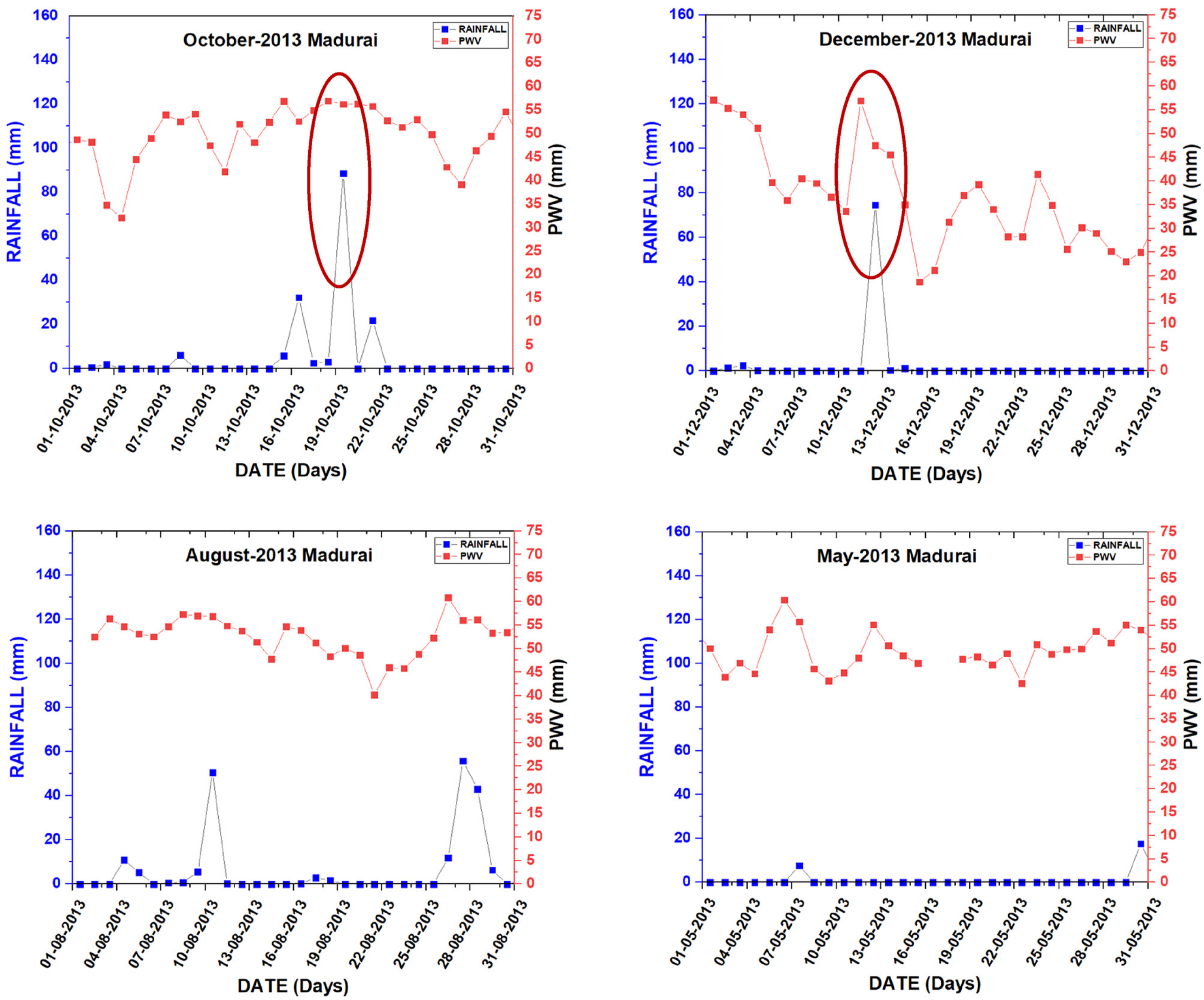

Figure 7: PWV and rainfall variation in Madurai.

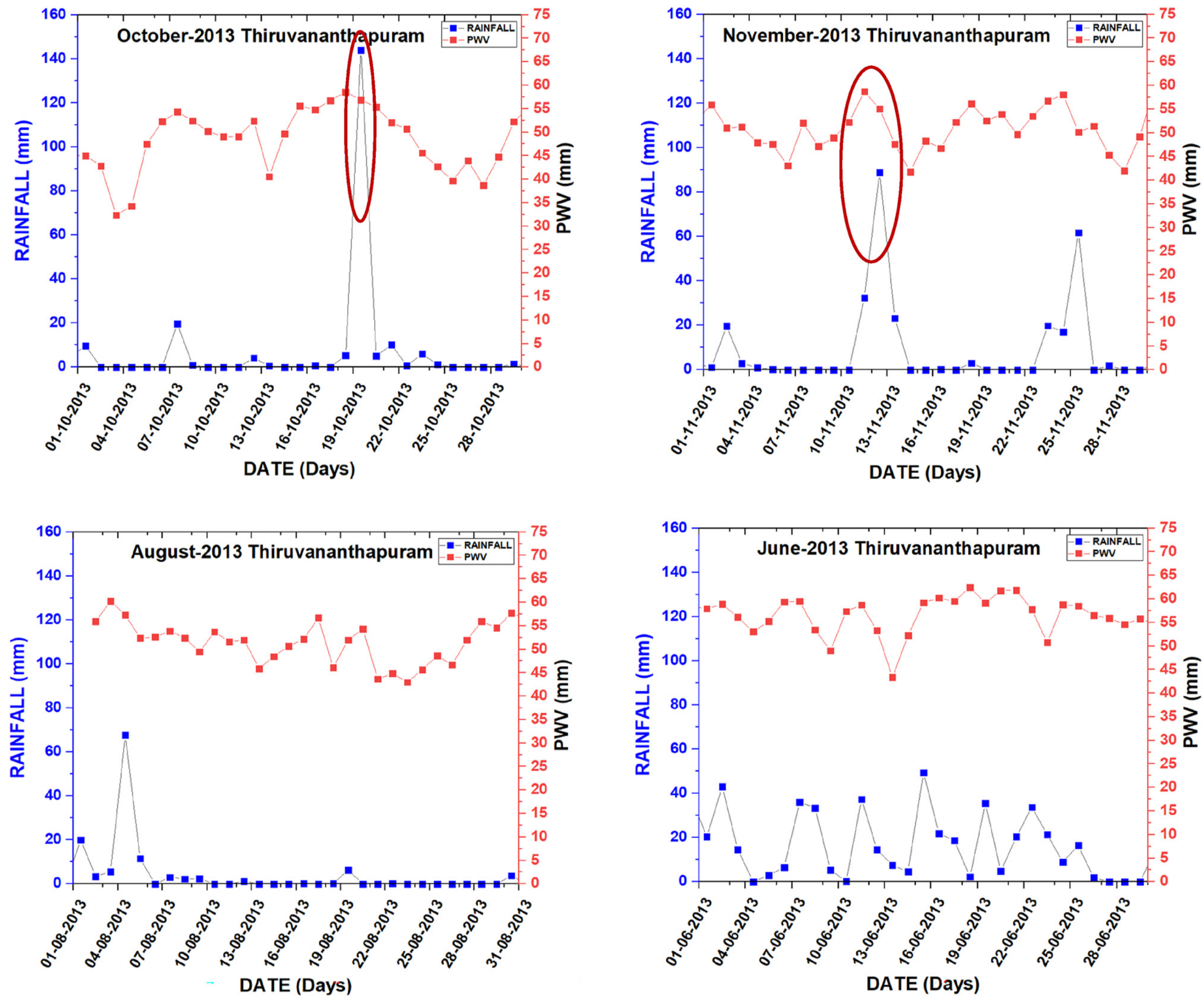

Figure 8: PWV and rainfall variation in Thiruvananthapuram.

Table 4: Change in PWV values comparison for different cities.

Rainfall place	DATE	Maximum PWV (mm)	Minimum PWV (mm)	ΔPWV (mm)	Interval (h)	Rate of change of PWV (mm/h)
Bangalore (1)	24-11-2013	38.42	24.7	13.72	13	1.05
Bangalore (4)	09-09-2013	43.24	40.41	2.83	23	0.12
Hyderabad (1)	10-10-2013	48.26	41.81	6.45	4	1.61
Hyderabad (2)	12-07-2013	56.69	49.82	6.87	16.3	0.42
Guwahati (1)	23-06-2013	71.62	66.06	5.56	6.3	0.88
Guwahati (2)	04-10-2013	62.92	59.21	3.71	8	0.46
Thiruvananthapuram (1)	20-10-2013	59.74	54.78	4.96	15.3	0.32
Thiruvananthapuram (2)	13-11-2013	62.96	45.05	17.91	23.3	0.77
Madurai (1)	20-10-2013	58.87	54.7	4.17	15	0.28
Madurai (2)	13-12-2013	54.44	41.55	12.89	22.3	0.58

(1) and (2) are two of the rainfall events observed, denoted by red circles in the above Figures 5–9 for the selected five cities. (4) In Bangalore the 4th highest rainfall event in the selected period. *In the above Figures 5–9, other than the top 2 rainfall events marked with red circles, the other rainfall events could be among the top 2 to seven rainfall events for that city, as the top 4 rainfall events may repeat in the same month.

5 Conclusions

This study provided an analysis of Precipitable Water Vapor (PWV) and rainfall variability across five Indian cities, Bangalore, Hyderabad, Guwahati, Thiruvananthapuram, and Madurai, using satellite observations from March 2013 to February 2014, except for Bangalore, where data were collected from April 2013 to February 2014. The observations revealed significant seasonal and diurnal variations in PWV and rainfall across these cities. Significant rainfall events showed rapid increases in PWV, followed by decreases post-rainfall. Bangalore had the highest PWV variation in September 2013 (44.16 mm) and the lowest in December 2013 (4.26 mm), with peak rainfall in November 2013 (108.40 mm). Hyderabad's highest PWV fluctuation occurred in July 2013 (56.14 mm), with maximum rainfall in October 2013 (98.30 mm). It was observed that Guwahati had its peak PWV variation in June 2013 (71.68 mm), coinciding with the highest rainfall in June 2013 (121.30 mm), while Thiruvananthapuram had the highest PWV in May 2013 (63.98 mm) and the highest rainfall in October 2013 (143.90 mm). Madurai's highest PWV variation occurred in August 2013 (60.82 mm), and October 2013 had the highest rainfall (88.5 mm). During specific rainfall events in these cities, PWV fluctuated, dropping before rainfall, peaking during it, and decreasing afterward. The preliminary statistical analysis will be extended with more locations data to investigate the correlation between PWV and rainfall shortly.

Research ethics: Not applicable.
Informed consent: Not applicable.
Author contributions: All authors have accepted responsibility for the entire content of this manuscript and approved its submission.
Use of Large Language Models, AI and Machine Learning Tools: None declared.
Conflict of interest: The authors state no conflict of interest.
Research funding: None declared.
Data availability: Not applicable.

References

1. Bevis M, Businger S, Herring TA, Rocken C, Anthes RA, Ware RH. GPS meteorology: remote sensing of atmospheric water vapor using the global positioning system. J Geophys Res Atmos 1992;97:15787–801.
2. Vey S, Dietrich R, Rülke A, Fritsche M, Steigenberger P, Rothacher M. Validation of precipitable water vapor within the NCEP/DOE reanalysis using global GPS observations from one decade. J Clim 2010;23:1675–95.
3. Smith TM, Arkin PA. Improved historical analysis of oceanic total precipitable water. J Clim 2015;28:3099–121.
4. Yao Y, Shan L, Zhao Q. Establishing a method of short-term rainfall forecasting based on GNSS-derived PWV and its application. Sci Rep 2017;7:12465.
5. Li X, Long D. An improvement in accuracy and spatiotemporal continuity of the MODIS precipitable water vapor product based on a data fusion approach. Rem Sens Environ 2020;248:111966.
6. Zhang B, Yao Y. Precipitable water vapor fusion based on a generalized regression neural network. J Geod 2021;95:36.
7. Ding J, Chen J, Tang W, Song Z. Spatial–temporal variability of global GNSS-derived precipitable water vapor (1994–2020) and climate implications. Remote Sens 2022;14:3493.
8. Li H, Wang X, Wu S, Zhang K, Chen X, Qiu C, et al. Development of an improved model for prediction of short-term heavy precipitation based on GNSS-derived PWV. Remote Sens 2020;12:4101.
9. Fontaine B, Roucou P, Trzaska S. Atmospheric water cycle and moisture fluxes in the West African monsoon: mean annual cycles and relationship using NCEP/NCAR reanalysis. Geophys Res Lett 2003;30. https://doi.org/10.1029/2002gl015834.
10. Wang H, Wei M, Li G, Zhou S, Zeng Q. Analysis of precipitable water vapor from GPS measurements in Chengdu region: distribution and evolution characteristics in autumn. Adv Space Res 2013;52:656–67.
11. Pacione R, Fionda E, Ferrara R, Lanotte R, Sciarretta C, Vespe F. Comparison of atmospheric parameters derived from GPS, VLBI and a ground-based microwave radiometer in Italy. Phys Chem Earth, Parts A/B/C 2002;27:309–16.
12. Kern A, Bartholy J, Borbás ÉE, Barcza Z, Pongrácz R, Ferencz C. Estimation of vertically integrated water vapor in Hungary using MODIS imagery. Adv Space Res 2008;41:1933–45.
13. Renju R, Suresh Raju C, Mathew N, Antony T, Krishna Moorthy K. Microwave radiometer observations of interannual water vapor variability and vertical structure over a tropical station. J Geophys Res Atmos 2015;120:4585–99.
14. Gui K, Che H, Chen Q, Zeng Z, Liu H, Wang Y, et al. Evaluation of radiosonde, MODIS-NIR-Clear, and AERONET precipitable water vapor using IGS ground-based GPS measurements over China. Atmos Res 2017;197:461–73.
15. Zhang W, Lou Y, Huang J, Zheng F, Cao Y, Liang H, et al. Multiscale variations of precipitable water over China based on 1999–2015 ground-based GPS observations and evaluations of reanalysis products. J Clim 2018;31:945–62.
16. Zhao Q, Ma X, Yao W, Liu Y, Yao Y. A drought monitoring method based on precipitable water vapor and precipitation. J Clim 2020;33:10727–41.
17. Suparta W, Zainudin SK. Precipitation analysis using GPS meteorology over antarctic Peninsula. In: 2015 International Conference on Space Science and Communication (IconSpace). Langkawi: IEEE; 2015:493–7 pp.

18. Rocken C, HovE TV, Johnson J, Solheim F, Ware R, Bevis M, et al. GPS/STORM—GPS sensing of atmospheric water vapor for meteorology. J Atmos Ocean Technol 1995;12:468−78.
19. Haase JS, Vedel H, Ge M, Calais E. GPS zenith tropospheric delay (ZTD) variability in the Mediterranean. Phys Chem Earth Solid Earth Geodes 2001;26:439−43.
20. Haase J, Ge M, Vedel H, Calais E. Accuracy and variability of GPS tropospheric delay measurements of water vapor in the western Mediterranean. J Appl Meteorol 2003;42:1547−68.
21. Zhang F, Barriot JP, Xu G, Yeh TK. Metrology assessment of the accuracy of precipitable water vapor estimates from GPS data acquisition in tropical areas: the Tahiti case. Remote Sens 2018;10:758.
22. Li X, Dick G, Lu C, Ge M, Nilsson T, Ning T, et al. Multi-GNSS meteorology: real-time retrieving of atmospheric water vapor from BeiDou, Galileo, GLONASS, and GPS observations. IEEE Trans Geosci Rem Sens 2015;53:6385−93.
23. Rivera Y, Capacete KC, Rodriguez SK, David AR, Macalalad E. Variations of precipitable water vapor from 2012 to 2019 over the Philippines using radiosondes. In: IOP Conference Series: Earth and Environmental Science. Malaysia: IOP Publishing; 2021, 880:012001 p.
24. Domingo AL, Macalalad EP. Multi-year precipitable water vapor observations in East Manila, Philippines using radiosonde and global navigation satellite system. In: E3S Web of Conferences. Shangai: EDP Sciences; 2020, 199:00002 p.
25. Saha K, Raju CS, Parameswaran K. A new hydrostatic mapping function for tropospheric delay estimation. J Atmos Sol Terr Phys 2010;72:125−34.
26. Jadala NB, Sridhar M, Dashora N, Dutta G. Annual, seasonal and diurnal variations of integrated water vapor using GPS observations over Hyderabad, a tropical station. Adv Space Res 2020;65:529−40.
27. Jade S, Vijayan MS. GPS-based atmospheric precipitable water vapor estimation using meteorological parameters interpolated from NCEP global reanalysis data. J Geophys Res Atmos 2008;113. https://doi.org/10.1029/2007jd008758.
28. Tomar CS, Bhatla R, Singh NL, Kumar V, Rai PK, Soni VK, et al. Evaluation of atmospheric precipitable water vapour distribution and trend over India. Theor Appl Climatol 2024;155: 8361−77.
29. Rani S, Maharana P, Mal S. Assessing the monthly trends in precipitable water vapor over the Indian subcontinent. Ann Am Assoc Geogr 2024;114:671−96.
30. Jadala NB, Sridhar M, Ratnam DV, Tummala SN. Ensemble based deep learning model for prediction of integrated water vapor (IWV) using GPS and meteorological observations. J Appl Geodesy 2024;18:253−65.